Rotation Invariant Co-occurrence among Adjacent LBPs

Ryusuke Nosaka, Chendra Hadi Suryanto, and Kazuhiro Fukui

Graduate School of Systems and Information Engineering,
Department of Computer Science, University of Tsukuba, Japan
{nosaka,chendra}@cvlab.cs.tsukuba.ac.jp,
kfukui@cs.tsukuba.ac.jp

Abstract. In this paper, we propose a new type of local binary pattern (LBP)-based feature, called *Rotation Invariant Co-occurrence among adjacent LBPs* (RIC-LBP), which simultaneously has characteristics of rotation invariance and a high descriptive ability. LBP was originally designed as a texture description for a local region, called a micropattern, and has been extended to various types of LBP-based features. In this paper, we focus on Co-occurrence among Adjacent LBPs (CoALBP). Our proposed feature is enabled by introducing the concept of rotation equivalence class to CoALBP. The validity of the proposed feature is clearly demonstrated through comparisons with various state-of-the-art LBP-based features in experiments using two public datasets, namely, the HEp-2 cell dataset and the UIUC texture database.

1 Introduction

The Local Binary Pattern (LBP) histogram has recently attracted much attention in the area of image recognition. The basic idea behind the LBP histogram is to represent an entire image as a histogram of numerous LBPs, with each LBP extracted from a local region of the image. Many types of LBP-based features [1–5] have been proposed as extensions of the original LBP.

In this paper, we propose a new type of LBP-based feature, which is invariant to rotation of an input image. The proposed feature is an extension of Co-occurrence among Adjacent LBPs (CoALBP) [6], which is an LBP-based feature with a higher descriptive ability than the original LBP. LBP was originally designed as a texture description for a local region, called a micropattern, which consists of binary patterns that represent the magnitude relation between the center pixel of a local region and its neighboring pixels. LBP is obtained by thresholding the image intensity of the surrounding pixels with that of the center pixel. To obtain an LBP histogram feature for use in classification, the binary patterns are converted to decimal numbers as labels, and then a histogram is generated from the labels of all the local regions of an entire image. The main advantage of LBP is its invariance to uniform changes in image intensity over an entire image, making it robust against changes in illumination. This is because LBP considers only the magnitude relation between the center and neighboring pixel intensities. Owing
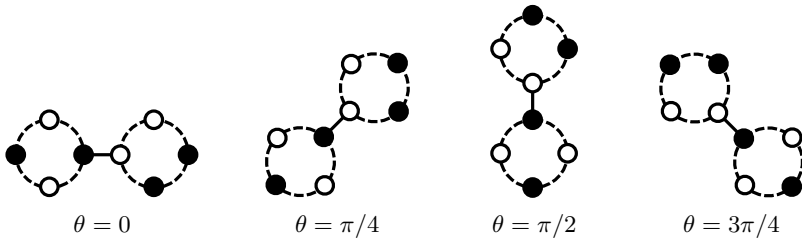
Fig. 1. Example of rotation equivalence class of LBP pairs. In this figure, each circle indicates one LBP.

to this characteristic, LBP has become a standard feature for texture recognition, face recognition, and facial expression analysis [1, 5].

To enhance the descriptive ability of LBP, the feature has been extended to CoALBP by introducing the concept of co-occurrence among LBPs so as to extract information related to the more global structures of the input image [6]. However, the CoALBP feature can vary significantly depending on the orientation of the target object. When, for instance, classifying several types of cells with complicated textures, rotation invariance is essential. This is because the orientation of each cell is not relevant to its classification. One could address this problem by preparing all possible LBPs in advance. However, this solution would entail a large memory requirement (to hold the reference patterns) high computational cost.

Several LBP-based features with rotation invariance have already been proposed. They are categorized into two types. The first type focuses on invariance to local rotation of an input image. For example, LBP^{ri} and LBP^{riu2} [4] obtain invariance to local rotation by introducing the concept of rotation equivalence class. The second type focuses on invariance to global rotation. The LBP-HF feature is included in this type. It attains global rotation invariance by applying the discrete Fourier transform to a feature vector of an LBP histogram [7]. Both types can extract distinctive features from an image with rotations. However, these rotation invariant features lack descriptive ability, because they are basically the local features extracted from only micro patterns, without consideration of the relations among micropatterns.

To overcome the problem of low descriptive ability of conventional rotation invariant LBPs, we incorporate the concept of rotation equivalence class into CoALBP. Fig.1 shows an example of the rotation equivalence class of CoALBPs. In this case, we consider that all CoALBPs corresponding to a different angle θ have the same value. Nevertheless, finding such LBP pairs is difficult since the number of possible LBP combinations is huge. To solve this problem, we automatically detect pairs with the same CoALBP value by using a computational algorithm. We call this feature *Rotation Invariant Co-occurrence among adjacent LBPs* (RIC-LBP). RIC-LBP can simultaneously provide a high descriptive ability and invariance to image rotation. The core idea of RIC-LBP is simple yet effective. The validity of RIC-LBP is demonstrated by comparing various
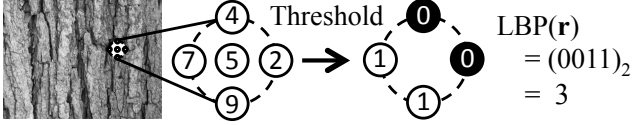
Fig. 2. Flow to obtain LBP from a local region. In this example, the intensity of the center pixel is 5 and those of its neighboring pixels are 2, 4, 7 and 9. Thus, the binary pattern is "0011" and $LBP(\mathbf{r}) = 3$.

state-of-the-art LBP-based features through the experiments using two public datasets, the HEp-2 cell dataset and the UIUC texture database.

The remainder of this paper is organized as follows. In Section 2, we briefly review LBP and co-occurrence among adjacent LBPs. In Section 3, we describe how to impart rotation invariance to CoALBPs. We also explain the RIC-LBP process. In Section 4, we demonstrate the validity of the proposed feature by examining the results of experiments in cell classification and texture recognition using public databases. In the final section, we present our conclusions.

2   LBP and Co-occurrence of Adjacent LBPs

2.1   LBP

LBP[3] is an operator that describes a local region as a binary pattern obtained by thresholding the difference between a center pixel and its neighboring pixels in a local region, as shown in Fig.2. The binary pattern in LBP represents the magnitude relation of intensities, a quantity which is invariant amid uniform changes of image intensity over an entire image. Therefore, LBP is robust against changes in illumination among image patterns, a difficulty commonly found in face and texture images.

Let I be an image intensity and $\mathbf{r} = (x, y)$ be a position vector in I. LBP at $\mathbf{r}$ is defined as follows:

$$LBP(\mathbf{r}) = \sum_{i=0}^{N-1} sgn(I(\mathbf{r} + \Delta\mathbf{s}_i) - I(\mathbf{r}))2^i, \tag{1}$$

$$sgn(x) = \begin{cases} 1, \text{ if } x \geq 0 \\ 0, \text{ otherwise} \end{cases}, \tag{2}$$

where N is the number of neighbor pixels. $\Delta\mathbf{s}_i$ is displacement vector from the center pixel to neighboring pixels given by $\Delta\mathbf{s}_i = (s\cos(\theta_i), s\sin(\theta_i))$, where $\theta_i = \frac{2\pi}{N}i$ and s is a scale parameter of LBP.

2.2   Co-occurrence among Adjacent LBPs

The original LBP does not preserve structural information among binary patterns, even though such information may be characteristic of an image. In order
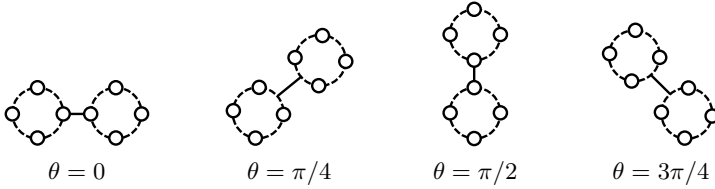
Fig. 3. Configurations of an LBP pair

to keep such structural information, we utilize the CoALBP as represented by LBP pair [6]. The set of CoALBPs over a whole image is converted to a CoALBP histogram feature. CoALBP (LBP pair) at $\mathbf{r}$ is written as follows:

$$P(\mathbf{r}, \Delta\mathbf{r}) = (LBP(\mathbf{r}), LBP(\mathbf{r} + \Delta\mathbf{r})), \tag{3}$$

where $\Delta\mathbf{r} = (r\cos\theta, r\sin\theta)$ is a displacement vector between an LBP pair. The value of r is an interval between an LBP pair, and $\theta = 0, \pi/4, \pi/2, 3\pi/4$. Fig.3 illustrates the configurations of an LBP pair.

While the LBP produces $2^N (= N_P)$ different output values, the number of possible combination patterns of an LBP pair $N_P^2 \times 4$ is significantly greater than that of the LBP itself. That is, an LBP pair can represent a far greater variety of image patterns than an LBP. The histogram feature generated from these LBP pairs contains information on the structure of the image, since it describes the frequency of LBP pairs that are located near each other.

3   Rotation Invariant Co-occurrence among Adjacent LBPs

3.1   Rotation Equivalence Class of LBP Pair

To simultaneously achieve a high descriptive ability and rotation invariance, we incorporate rotation invariance into CoALBP as represented by an LBP pair. The simplest way to embed rotation invariance is to attach a rotation invariant label to each LBP pair. For example, in Fig.4 there are two types of LBP pairs, each having four configurations. The same label is attached to each of these eight LBP pairs because each LBP pair is equal to the others in terms of rotation. This relation among LBP pairs is called rotation equivalence; and a set of rotation equivalent LBP pairs is called a rotation equivalence class of LBP pairs. Thus, the LBP pairs in Fig.4 constitute one rotation equivalence class.

As shown in Fig.4, the upper LBP pairs are equivalent to LBP pairs that have been rotated 180 degrees from the lower LBP pairs. Therefore, for finding the rotation equivalent LBP pairs, it is necessary to consider only two cases: (i) a case in which LBP pairs of $\theta = 0, \pi/4, \pi/2, 3\pi/4$ have rotation equivalence and (ii) a case in which LBP pairs that are rotated by 180 degrees have rotation equivalence.
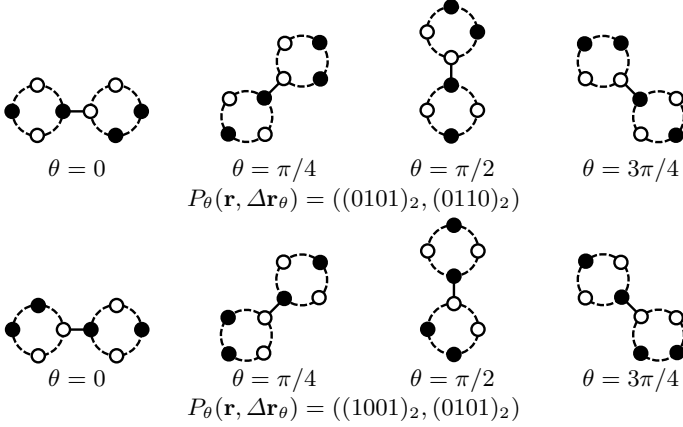
Fig. 4. An example of the rotation equivalence class. The same label is attached to these LBP pairs.

First, in order to consider case (i), we modify the definition of LBP pair. The modified LBP pair is written as follows:

$$P_\theta(\mathbf{r}, \Delta\mathbf{r}_\theta) = (LBP_\theta(\mathbf{r}), LBP_\theta(\mathbf{r} + \Delta\mathbf{r}_\theta)), \tag{4}$$

$$LBP_\theta(\mathbf{r}) = \sum_{i=0}^{N-1} sgn(I(\mathbf{r} + \Delta\mathbf{s}_{i,\theta}) - I(\mathbf{r}))2^i, \tag{5}$$

$$\Delta\mathbf{s}_{i,\theta} = (s\cos(\theta_i + \theta), s\sin(\theta_i + \theta)), \tag{6}$$

where θ serves as the bias of the rotation angle in LBP. Based on the new definition above, the LBP pair of each configuration has the same value in terms of rotation.

Next, we consider case (ii). In this case, we use a rule that an LBP pair that is rotated 180 degrees from $P_\theta(\mathbf{r}, \Delta\mathbf{r}_\theta)$ is equal to $(LBP_{\theta+\pi}(\mathbf{r} + \Delta\mathbf{r}_\theta), LBP_{\theta+\pi}(\mathbf{r}))$. According to this rule, we can consider that these LBP pairs have rotation equivalence. We implement this rule by a mapping table M that has a label for each LBP pair. The mapping table M is generated by using Algorithm 1. In Algorithm 1, "$\gg$" is a circular shift ; also, "$i' = i \gg N/2$" means to rotate LBP i by 180 degree (e.g., $i = (1000)_2$ becomes $i' = (0010)_2$).

By using mapping table M, we define a rotation invariant label for an LBP pair at $\mathbf{r}$ (i.e., RIC-LBP) as follows:

$$P_\theta^{RI}(\mathbf{r}) = M(P_\theta(\mathbf{r}, \Delta\mathbf{r}_\theta)). \tag{7}$$

Finally, an RIC-LBP histogram is generated from $P_\theta^{RI}(\mathbf{r})$ for the entire image.

Since the number of the rotation equivalence classes for the LBP pairs determines the dimension of the RIC-LBP histogram vector, we describe this in more

---

Algorithm 1. Calculate a mapping table M

Input: N // number of neighbor pixels.
Output: M // mapping table ($N_P \times N_P$ matrix)
   $id \Leftarrow 1, N_P \Leftarrow 2^N$
   for $i = 0, \cdots, N_P - 1$ **do**
     for $j = 0, \cdots, N_P - 1$ **do**
       if $M(i, j) = null$ **then**
         $i' \Leftarrow i \gg N/2, \quad j' \Leftarrow j \gg N/2$
         $M(i, j) \Leftarrow id, \quad M(j', i') \Leftarrow id$
         $id \Leftarrow id + 1$
       end if
     end for
   end for
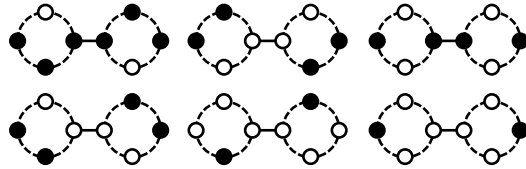
Fig. 5. Examples of symmetric LBP pair

detail as follows. The number of possible LBP pairs is $N_P^2 \times 4$. By considering case (i), the number of possible patterns becomes N_P^2. Moreover, by considering case (ii), the number of possible patterns is halved. Here, we consider a symmetric LBP pair as shown in Fig.5; the number of symmetric LBP pairs is N_P. Therefore, the number of rotation equivalence classes is $N_P(N_P + 1)/2$.

3.2   Process Flow of Generating RIC-LBP Histogram from an Image

We explain how to generate the RIC-LBP histogram from an input image with Eq.(4) and mapping table M.

First, we explain how Eq.(4) and mapping table M work using Fig.6. The example image has four LBPs (Fig.6(a)). The image is decomposed into six LBP pairs (Fig.6(b)). We then have two sets of LBP pairs that have rotation equivalence as indicated by arrows in Fig.6(b). By Eq.(4), the effect of configurations is removed from these LBP pairs, as shown in Fig.6(c). By utilizing mapping table M, these pairs are arranged as shown in Fig.6(d). As we can see, LBP pairs in Fig.6(d) are clearly rotation invariant. By such a process, we obtain an RIC-LBP histogram of the example image, as shown in Fig.6(e).

Next, we explain the overall process flow to obtain a RIC-LBP histogram of an image using Fig.7. Firstly, compute $LBP_\theta(\mathbf{r})$ at every pixel $\mathbf{r}$ throughout the entire input image (Fig.7(a)). Next, compute a histogram of $P_\theta(\mathbf{r}, \Delta\mathbf{r}_\theta)$ (Fig.7(b)). Finally, combine the histogram using mapping table M and obtain a histogram
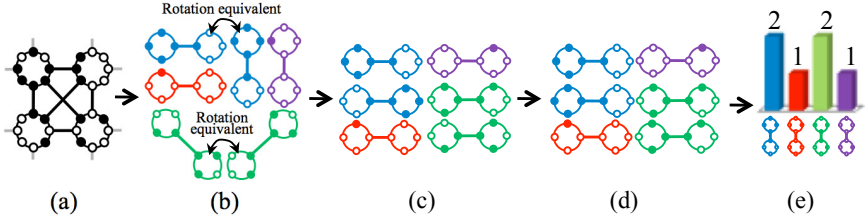
Fig. 6. An example of generating RIC-LBP. (a) Example image. (b) LBP pairs of the example image. (c) Labeling of each LBP pair using Eq.(4). (d) Re-labeling of each LBP pair by applying the mapping table M. (e) RIC-LBP histogram.
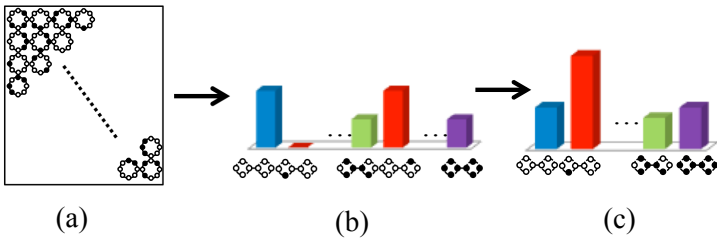

Fig. 7. Process flow of RIC-LBP. (a) Input LBP image. (b) Histogram of $P_\theta(\mathbf{r}, \Delta\mathbf{r}_\theta)$. (c) Histogram of $P_\theta^{RI}(\mathbf{r})$.

of $P_\theta^{RI}(\mathbf{r})$ (Fig.7(c)). Mapping table M is calculated offline. The final histogram is $N_P(N_P + 1)/2$ dimensional vector and is applied to a classifier.

4 Experiments

To evaluate the effectiveness of RIC-LBP, we conducted two types of experiments. The first experiment is for HEp-2 cells classification, an important task to support autoimmune disease diagnosis. Experimental conditions and results are presented in Section 4.1. The second experiment is to apply RIC-LBP to compare its performance relative to other LBP features in general texture recognition, which is described in Section 4.2.

4.1 HEp-2 Cells Classification

Setup. In this experiment, we used the HEp-2 cell dataset from the classification contest at ICPR 2012 [8]. The dataset contains six kinds of antinuclear antibody (ANA) patterns of HEp-2 cell images: *homogeneous*, *fine speckled*, *coarse speckled*, *centromere*, *cytoplasmatic*, and *nucleolar*, as shown in Fig.8. The total number of images in the dataset is 648. The images are of various sizes.
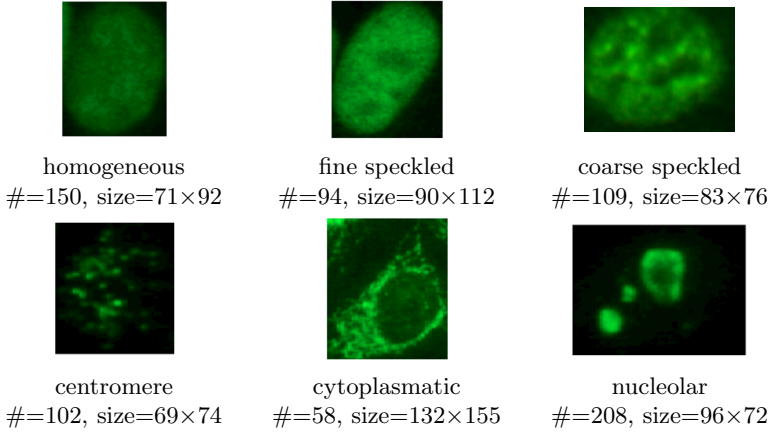
homogeneous
#=150, size=71×92

fine speckled
#=94, size=90×112

coarse speckled
#=109, size=83×76

centromere
#=102, size=69×74

cytoplasmatic
#=58, size=132×155

nucleolar
#=208, size=96×72

Fig. 8. Example images in Hep-2 cell dataset. # is the number of images of each class. "size" is the size of the displayed image; other images not displayed have different sizes.
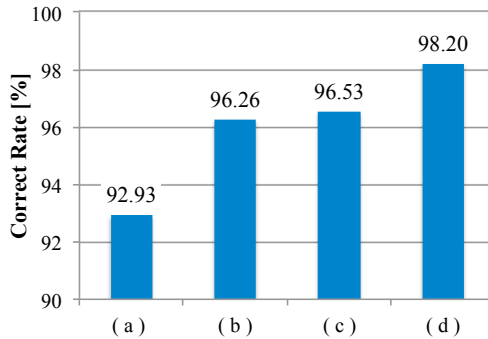

Fig. 9. Performance results. (a) LBP histogram, (b) rotation invariant LBP histogram, (c) LBP pair histogram (CoALBP), (d) rotation invariant LBP pair histogram (RIC-LBP, proposed).

We employed the leave-one-out protocol for evaluation; the correct rate is reported as our experimental result. The parameters of RIC-LBP were set as follows. The radius of LBP was set to $s = 1, 2, 4$ pixels and the intervals of LBP pairs were set to $r = 2, 4, 8$ pixels. Then, the features extracted by each parameter were combined into a final proposed feature vector with dimension of 408 (=136 × 3). The parameters of other methods were also set to produce optimal performance. For classification, the linear SVM was used [9].

Result. First, we show the effectiveness of the proposed feature comparing with various conventional LBP histograms. The baseline result for the original LBP

Table 1. Performance results in HEp-2 cells classification

Method	Correct Rate(%)
LBP^{ri} [4]	96.26
LBP^{riu2}[4]	76.67
LBP-HF [7]	97.23
RIC-LBP (Proposed)	98.20

histogram was 92.93% (Fig.9(a)). When we applied the method with rotation invariance, the correct rate rose to 96.26% (Fig.9(b)). The co-occurrence of adjacent LBPs (i.e. CoALBP) achieved a performance of 96.53% (Fig.9(c)). When we used the proposed RIC-LBP, the performance was further improved to 98.20% (Fig.9(d)). Finally, the proposed method significantly improved the performance of the original LBP by more than 5%. This result demonstrates the effectiveness of both the high descriptive ability of the CoALBPs and the rotation invariance in cell classification.

Next, we compare the results of RIC-LBP with those of other rotation invariant LBP features, as shown in Table 1. As apparent with the experimental results, RIC-LBP outperforms the other methods. These results confirm the significant advantage of RIC-LBP over the conventional methods, especially because the proposed method has not only rotation invariance, but also a high descriptive ability due to CoALBPs.

4.2   Texture Recognition

Setup. We evaluated RIC-LBP for texture recognition using the UIUC texture database [10]. The database contains texture images of 25 classes. Each class consists of 40 images of size 640×480 pixels. Some examples of texture images are shown in Fig.10. The images of each class were randomly split into training and testing sets. This division was repeated 20 times to produce 20 evaluation sets. The average of all correct rates over 20 iterations was defined as the final rate. To increase the difficulty of recognition, we also rotated the texture images by various angles. The parameters of the LBP features were set to the same setting as in the above mentioned experiment.

Results. Experimental results are shown in Table 2. The performance of RIC-LBP was better than that of almost all the other conventional LBP methods, such as LBP^{ri} and LBP^{riu2}. However, the LBP-HF method, which utilizes the discrete Fourier transform, achieved better performance than RIC-LBP. This is because RIC-LBP considers rotation at local regions, whereas LBP-HF considers rotation of the entire image. LBP-HF is thus better suited for this type of texture dataset, which contains global rotation equivalence images. This experimental result indicates that the performance of RIC-LBP for the texture dataset may be further improved by also considering rotation of the entire image by using a method such as the discrete Fourier transform.
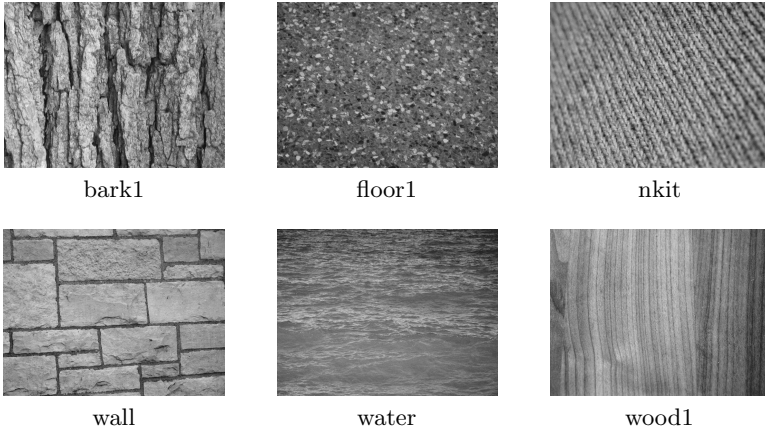
bark1   floor1   nkit

wall   water   wood1

Fig. 10. Example images in UIUC texture database

Table 2. Performance results in texture recognition

Method	Correct Rate(%)
LBP[3]	82.55
LBP^{ri} [4]	83.51
LBP^{riu2}[4]	57.33
CoALBP [6]	81.49
LBP-HF [7]	93.60
RIC-LBP (Proposed)	88.27

5   Conclusion

In this paper, we proposed RIC-LBP, a new type of LBP-based feature that simultaneously has the characteristics of rotation invariance and high descriptive ability. Conventional rotation invariant LBP-based features lack descriptive ability. To solve this problem, we focused on CoALBP, which is one effective extension of LBP. Compared with the original LBP, CoALBP has higher descriptive ability since it considers the global relation among LBPs. The proposed RIC-LBP obtained rotation invariance by introducing rotation equivalence class to the CoALBP. The validity of RIC-LBP, in particular, its robustness against local rotations due to transformations of target objects, was confirmed through classification experiments with cells and textures using public databases, specifically the HEp-2 cell dataset and the UIUC texture database.

References

1. Lei, Z., Liao, S., He, R., Pietikäinen, M., Li, S.: Gabor volume based local binary pattern for face representation and recognition. In: Proc. of IEEE International Conference on Automatic Face and Gesture Recognition, pp. 1–6 (2008)

2. Liu, C., Wechsler, H.: Gabor feature based classification using the enhanced fisher linear discriminant model for face recognition. IEEE Trans. on Image Processing 11, 467–476 (2002)
3. Ojala, T., Pietikäinen, M., Harwood, D.: A comparative study of texture measures with classification based on featured distributions. Pattern Recognition 29, 51–59 (1996)
4. Ojala, T., Pietikäinen, M., Mäenpää, T.: Multiresolution gray-scale and rotation invariant texture classification with local binary patterns. IEEE Trans. on Pattern Analysis and Machine Intelligence 24, 971–987 (2002)
5. Zhang, B., Gao, Y., Zhao, S., Liu, J.: Local derivative pattern versus local binary pattern: face recognition with high-order local pattern descriptor. IEEE Trans. on Image Processing 19, 533–544 (2010)
6. Nosaka, R., Ohkawa, Y., Fukui, K.: Feature Extraction Based on Co-occurrence of Adjacent Local Binary Patterns. In: Ho, Y.-S. (ed.) PSIVT 2011, Part II. LNCS, vol. 7088, pp. 82–91. Springer, Heidelberg (2011)
7. Ahonen, T., Matas, J., He, C., Pietikäinen, M.: Rotation Invariant Image Description with Local Binary Pattern Histogram Fourier Features. In: Salberg, A.-B., Hardeberg, J.Y., Jenssen, R. (eds.) SCIA 2009. LNCS, vol. 5575, pp. 61–70. Springer, Heidelberg (2009)
8. Contest on HEp-2 cells classification, `http://mivia.unisa.it/hep2contest`
9. Fan, R., Chang, K., Hsieh, C., Wang, X., Lin, C.: LIBLINEAR: A library for large linear classification. The Journal of Machine Learning Research 9, 1871–1874 (2008)
10. Lazebnik, S., Schmid, C., Ponce, J.: A sparse texture representation using local affine regions. IEEE Trans. on Pattern Analysis and Machine Intelligence 27, 1265–1278 (2005)